COBEM 2021 26th International Congress of Mechanical Engineering
November 22-26, 2021, Virtual Congress, Brazil

COB-2021-0120
SIMULATION AND ANALYSIS OF A HORIZONTAL AXIS WIND TURBINE SUBJECT TO A TURBULENT WIND FIELD

Layse Freitas Boere de Moraes
Milton Dias Junior
Structures and Machinery Dynamics Laboratory. University of Campinas, Rua Mendeleyev, 200, Campinas, São Paulo.
layseboere@gmail.com; milton@fem.unicamp.br

Abstract. *The most effective strategy for reducing the production cost of wind power is to upscale wind turbines. Since the decade of 1980, the wind industry has been through a period of intense and fast transitions related to this upscale process, which is intrinsically associated with the feasibility of production cost. The unavoidable upscale of wind turbines generate serious vibrations problems which need to be studied not only to ensure the safety of operations under these conditions but also to provide higher power generation efficiency at low costs. This work aims to analyze the low-frequency vibrations behavior using a wind turbine elastic model with 13 DOF, exposed to a two-dimensional velocity field. The three blades are modeled by Bernoulli-Euler Beam theory, the system was modeled using modal approach and the technical specifications are provided by NREL offshore 5-MW Baseline Wind Turbine. The model periodic time-dependence was analyzed through impulse tests and application of the Multi-Blade Coordinate Transformation, this transformation was applied to filter the PSD periodic frequency and to solve the eigenvalue problem. The SANDIA Method was used to model the 2D turbulent wind velocity field, and the difference between the point of view in the spectra (space frame or rotational blade frame) is analyzed. Lastly, the forced vibration behavior, in which the aerodynamic force was provided by the 2D turbulent wind velocity field was simulated. The expressive coupling between the model degrees of freedom as well as its periodic time dependence is shown by the PSD results. All simulations performed in this work present a good agreement with the literature for simulated cases and field measures as well.*

Keywords: *Wind Energy; Horizontal Axis Wind Turbine, MBC-transformation; Low Frequency Vibratory Behavior; Modal Approach.*

1. INTRODUCTION

In In the last 20 years, wind energy has been developing and expanding in the energy market. Recently (up to 2019), it has established itself as a consolidated source of clean and cost-competitive energy. The world's energy matrix is quickly moving away from fossil fuel consumption, usually related to climate changes, towards cleaner and renewable forms of energy as an effort to reach the agreed-upon climate goals (IRENA, 2019). This tendency is also observed in Brazil, as reported by the Associação Brasileira de Energia Eólica (Brazilian Wind Energy Association), ABEEOLICA (ABEEólica, 2019).

In this scenario, the most effective strategy for reducing the production cost of wind power is the wind turbine upscale. Starting in the 1980s, the wind industry has been through a period of intense and fast transitions related to this upscale process, which is intrinsically associated with a lower production cost. The unavoidable upscale of wind turbines generate serious vibrations problems which need to be studied not only to ensure safe operation under these conditions but also to provide higher power generation efficiency at low costs.

This work aims to model, simulate, and analyze a large-scale wind turbine – which has a generating capacity of 5MW, 87 meters of the tower height, and 110 meters of rotor diameter - subjected to a turbulent wind field and operating under stable conditions and at a constant velocity, using a structural model idealized with 13 degrees of freedom and simulated by applying the modal approach.

2. STRUCTURAL MODEL

Th The structural model is based on the model initially proposed by Zhang (2015), in which a complete three-bladed horizontal axis wind turbine (containing tower, powertrain, and rotating blades) is idealized with 13 degrees of freedom (DOFs): six DOFs describing individual movements of each of three blades, five DOFs describing the tower's movements and two DOFs describing powertrain's movements. The system's equations of motion (EOM) are obtained applying the Modal Approach Method, also known as Generalized Displacement Discretization Method (Clough and Penzien,1975). Through this method, the physical parameters for the first 11 DOFs are approximated using the linear density and the

component's structural flexibility together with the shape functions that, in the case of this wind turbine model, are the structure's first vibration mode related to the degree of freedom of reference,

The 13 DOF aeroelastic model is shown in Figure 1. The tilt movement and the blades' conicity are neglected. Four coordinate systems are used to develop the wind turbine aeroelastic model, one being an inertial coordinate system and the others three are moving coordinate systems, each fixed to one of the three blades. Only one of the moving systems fixed to the blades is illustrated in Figure 1.

The first coordinate system, formed by the X_1, X_2, X_3, constitute the inertial coordinate system and has its origin at the base of the tower. Each of the other coordinate systems is fixed at the center of the hub and moves along with each blade. In Figure 1 this system is formed by x_1, x_2 e x_3 axes. The x_3 axis is positioned along of the undeformed blade and is oriented positively towards the blade tip. The X_1 and x_1 are collinear with each other and with the mean wind speed. The X_2 and X_3 axes are located at the rotor plane and the x_2 and x_3 axes coincide with the tower's mid plane. The position of the local coordinate system, which is coupled to blade b is specified by azimuth $\Psi_b(t)$; defined as positive clockwise when viewed from the downwind position (Zhang, 2015).

The three blades are modeled by Bernoulli-Euler's beam theory and are idealized as having only 2 degrees of freedom each: one in the blade's lateral direction, within the rotor plane, and the other in the blade's longitudinal direction, perpendicular to the rotor plane, both are defined in the local coordinate system of each blade. For the case of the blade b, being $b = 1,2,3$, its displacements are defined by the degrees of freedom $q_b(t)$ and $q_{b+3}(t)$, in which the first coordinate characterizes the flapwise motion, while the second, the edgewise motion.

The following five degrees of freedom, described in the global coordinate system, $q_7(t)$ to $q_{11}(t)$, refer to the tower's movement: $q_7(t)$ and $q_8(t)$ representing the tower displacement at the hub height, and $q_9(t)$, $q_{10}(t)$ and $q_{11}(t)$, the rotations on axes X_1, X_2 and X_3, respectively. The powertrain is idealized through two rotational degrees of freedom: $q_{12}(t)$ and $q_{13}(t)$, the former corresponding to the angular displacement of the hub and the latter to the angular displacement of the generator input. Two issues should be considered when analyzing these degrees of freedom: 1. The positive direction of the angular displacements must consider the number of gear transmission stages (planetary + gearbox), for even-numbered gearboxes stages, $q_{12}(t)$ and $q_{13}(t)$ have the same direction, and for odd-numbered gears, the directions are opposite; 2. It should be remembered that the angular displacement $q_{13}(t)$ is amplified when it is compared to $q_{12}(t)$, due to the gear ratio N of the transmission.

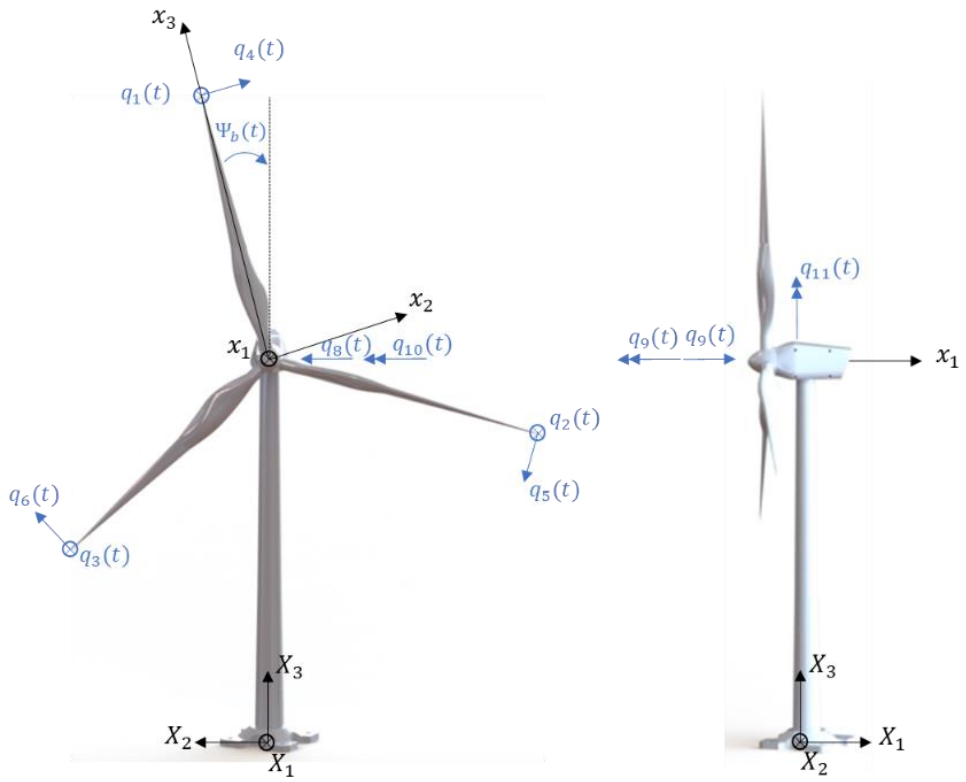

Figure 1. 13-DOF Aeroelastic wind turbine model

The azimuth angle is given by Equation 1:

$$\Psi_b(t) = \Omega t + {}^{2\pi}/_{3}\,(b-1) + q_{12}(t), \qquad b = 1,2,3 \tag{1}$$

The structure degrees of freedom can be summarized by:

$$\boldsymbol{q_l}(t) = \begin{bmatrix} q_1(t) \\ q_2(t) \\ q_3(t) \\ q_4(t) \\ q_5(t) \\ q_6(t) \end{bmatrix}, \quad \boldsymbol{q_g}(t) = \begin{bmatrix} q_7(t) \\ q_8(t) \\ q_9(t) \\ q_{10}(t) \\ q_{11}(t) \\ q_{12}(t) \\ q_{13}(t) \end{bmatrix} \tag{1}$$

3. MULTI-BLADE COORDINATE TRANSFORMATION

Wind turbines' dynamics are generally defined in two coordinate systems, where the blades' DOF are described in a rotating coordination system attached to them, while the tower, power train, and nacelle (nonrotational parts) are related DOF are described in a fixed coordinate system. The Multiblade Coordinate Transformation (MBC) or Coleman Transformation (Bir, 2008; 2010) is a special case of Lyapunov- Floquet Transformation for an isotropic rotor. MBC is a linear transformation that relates the rotating DOFs to new degrees of freedom fixed in the inertial frame i.e. converts the rotor's rotating coordinates to non-rotated ones (Skjoldan and Hansen, 2009). The azimuth equation – Eq. (3) – can be generalized as:

$$\Psi_b(t) = \Psi + \frac{2\pi}{N_{blades}}(b-1) \tag{3}$$

where Ψ_b is the blade azimuth angle, with $b = 1,2\ and\ 3$. The azimuth angle Ψ is 0 (zero) when the reference blade is in the upward vertical position.

Let q_b^g be the g-*th* DOF – which belongs to the rotational coordinate system – of the da b-*th* blade. The MBC related non-rotating new coordinates are as follows:

$$q_0^g = \frac{1}{3}\sum_{b=1}^{3} q_b^g \qquad q_c^g = \frac{2}{3}\sum_{b=1}^{3} q_b^g \cos\Psi_b \qquad q_s^g = \frac{2}{3}\sum_{b=1}^{3} q_b^g \sin\Psi_b \tag{4}$$

These new degrees of freedom are expressed in a nonrotating frame and are called "nonrotating degrees of freedom" (they can also be referred to as "rotor coordinates") and they express the cumulative behavior of the rotor – instead of the previous ones, which describe each individual blade behavior – in the global system. q_c^g is the cosine-cyclic mode and q_s^g is the sine-cyclic mode; these two modes together with the q_0^g led to the coupling of the rotor with the rest of the wind turbine.

The inverse transformation, yielding the blade coordinate given the rotor coordinates, is presented in Eq (5).

$$q_b^g = q_0^g + q_c^g \cos\Psi_b + q_s^g \sin\Psi_b, \qquad b = 1,2,3 \tag{5}$$

4. TURBULENT WIND FIELD SIMULATION

The wind simulation follows the SANDIA Method published by Veers (1988), which proposes the simulation of wind-speed time series for each specific point in the plane of the wind turbine rotor (which also is a plane perpendicular to the mean wind direction), which can be seen in Figure 2 on the left, so in this work, the number of samples in the radial direction represents the blade discretization (the radius of the circle is the length of the blades) and the number of samples in the circumferential direction is the spatial discretization of the movement of the blades in around the main rotor shaft.

Starting from a real turbulence power spectral density (PSD) and its coherence function – which describes how turbulence varies as a function of the spatial distance between the blades discretized points, the mean wind speed, and the frequency (Veers, 1988) – for each point in the turbulence field, an associated time-series signal is generated. Therefore, each time series is the excitation signal located in points of the rotor plane through which the blades pass during the rotation of the wind turbine rotor.

Using SANDIA Method, it is also possible to generate the turbulent velocity field in 3 dimensions, however, in the proposed structural model, the blades' conicity has been neglected, therefore, only 2 dimensions data (that define the rotor plane) are needed as input to the model.

Furthermore, generating a full-time series for each point on the turbulence field is a waste of computational resources, once, for each completed rotation of the rotor, the blades will only occupy one location of the azimuth angle at each time step. Therefore, each data point in the time series simulation is generated aiming to correspond to the exact time that the wind turbine blade occupies that point in space. Veers (1988) proposes the implementation of the time lag by shifting the phase of each frequency component in the PSD by the appropriate amount before transforming it into the time domain. Due to this rotational sampling, the spatial discretization is directly associated with the temporal discretization of the generated wind field data.

The wind turbulence model simulated in this work follows the IEC 61400 3rd edition standard (BSI Standards Publication – wind energy generation systems, 2019) and it is based on Kaimal PSD of turbulence that is shown in Figure 2 on the right.

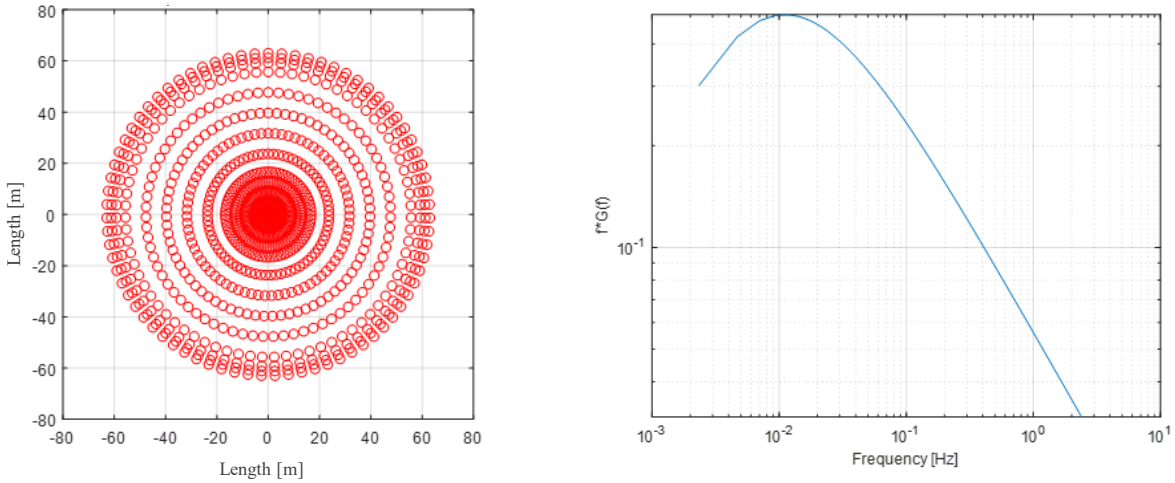

Figure 2. On the left, locations of points for wind simulation and on the right turbulence PSD by Kaimal.

5. CASE STUDY

5.1 Impulsive test

At first, impulsive tests were performed to understand the free vibration response of the system operating at its constant nominal rotation $\Omega = 12\,rpm$. The Multi-blade Coordinate Transformation has been applied before solving the eigenvalue problem and the of the natural frequencies for the operating wind turbine and they are shown in Table 1. The values referring to natural frequencies ± the machine's rotation frequency are also included in this table.

Table 1. Natural Frequencies in $\Omega = 12\,rpm$ and harmonics

$f_n + \Omega\ [Hz]$	$f_n\ [Hz]$	$f_n - \Omega\ [Hz]$
0,2000	0,0000	-0,2000
0,4697	0,2697	0,0697
0,5336	**0,3336**	**0,1336**
0,5391	0,3391	0,1391
0,6897	**0,4897**	**0,2897**
0,9007	**0,7007**	**0,5007**
1,0809	**0,8809**	**0,6809**
1,0913	0,8913	0,6913
1,4937	1,2937	1,0937

Figure 3 shows the result of the impulse test for a velocity condition applied in the degree of freedom of blade 1 in flapwise direction (no MBC). Analyzing the PSD presented in Figure 3, one can notice that for each natural frequency f_n, there are also two distant lateral components on the frequency axis, of $\pm\Omega$ from f_n. Thus, for each value of f_n, we can also identify components at $f_n + \Omega$ and $f_n - \Omega$.

The appearance of the side components around the natural frequency values is a characteristic of periodic systems and their variations over time. These components can also appear in the second multiple of the rotation ($\pm 2\Omega$) or even larger orders, the amplitudes of these components depend, among other factors, on the degree of rotor anisotropy (Hansen, 2016). The result in Figure 3 is in agreement with the results described by Skjoldan and Hansen (2009).

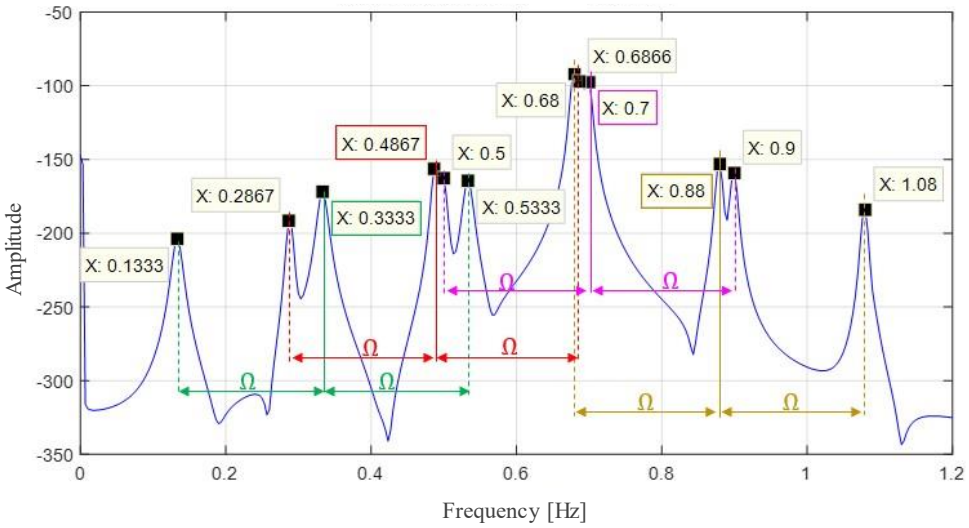

Figure 3. PSD of Blade 1 displacement at flapwise direction.

The application of the MBC transformation to the same impulse test yields the results shown in figure 4. Note that the harmonic components are filtered out exactly as described by Bir (2010).

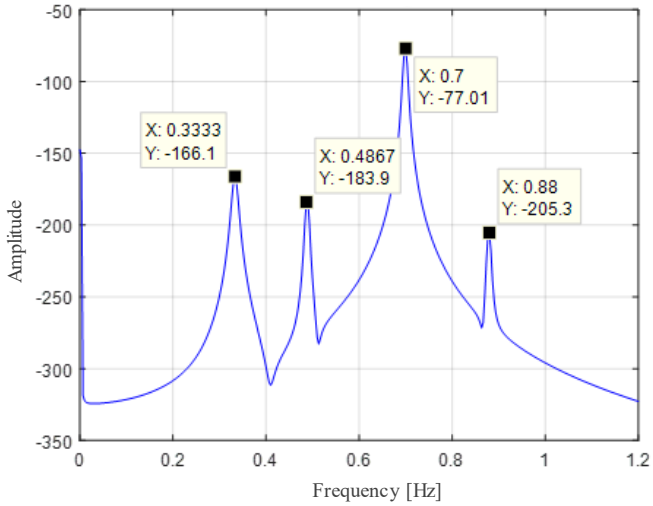

Figure 4. PSD of Blade 1 displacement after MBC application.

5.2 Structural model submitted to the 2D turbulent wind field

Once the wind velocity field was applied as excitation to the wind turbine model, the aerodynamic forces acted accelerating the rotor, as the pitch control was not included in the structural model, a resistive torque was applied in the generator aiming to keep the wind turbine rotation at its operational velocity Ω = 12 rpm.

The PSDs of the structural model subjected to the 2D wind turbulence field, which are shown in Figures 5 and 6, were obtained using the Hanning window and the MBC transformation was not applied. To facilitate the analysis of the spectral content of the wind turbine's response signals, Table 2 presents a code for each wind turbine's natural frequency and its value in operation as well.

Figure 5, on the left, presents the PSD of the torsional vibration of the rotor (coordinate $\dot{q}_{12}$), it is noticed that the system responds, predominantly, in the power train torsion, but it also responds in multiple harmonic components of the blade pass frequency, 3Ω. A similar effect was observed for all degrees of freedom described in the inertial reference system; this effect was also observed by Yang et *al.* (2014).

Table 2. Natural frequencies – $\Omega = 12rpm$

NAME	MODE	$f_n[Hz]$
PT	2nd Powertrain Torsion	0,2697
TFA	Tower fore-and-after	0,3336
TSS	Tower side-side	0,3391
FBW	1º *Flapwise* backward	0,4897
FS	1º *Flapwise* symmetric	0,7007
FFW	1º *Flapwise* forward	0,8809
EBW	1º *Edgewise* backward	0,8913
EFW	1º *Edgewise* forward	1,2937

On the right of Figure 5, it is shown the PSD of the tower fore-and-after. One can notice the coupling existing between the vibration modes of the wind turbine, the tower bending mode, the blade pass frequency (3Ω), and its multiples can be observed as well as the natural frequencies of the power train's torsion and blade's flapwise.

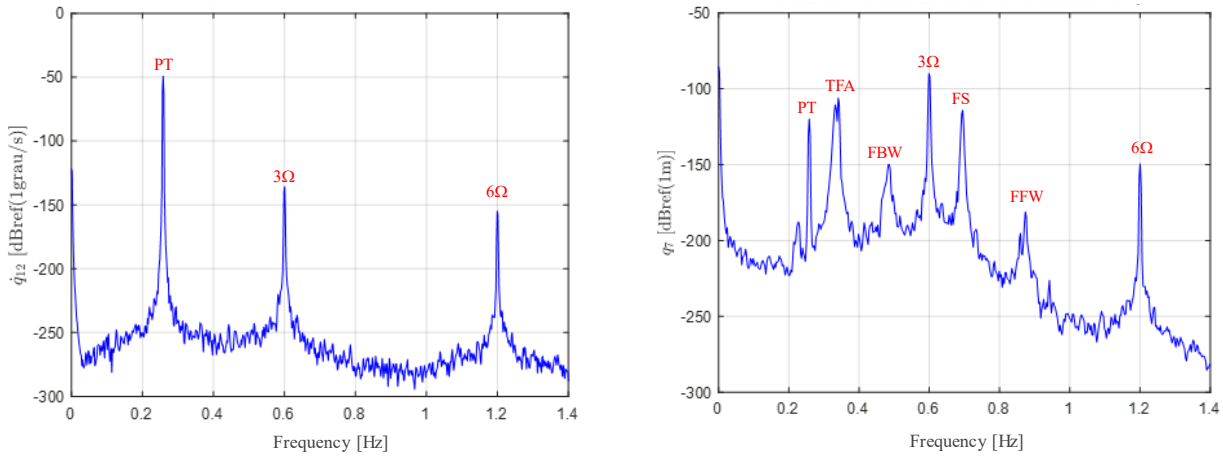

Figure 5. PSD of forced vibration response: on the left powertrain torsional and on the right tower fore-and-after.

Figure 6 shows the PSDs associated with the Blade 1 flapwise and edgewise DOFs, on the left and the right, respectively. It shows a significant number of harmonic components in those PSDs, it is possible to identify some peaks associated with the natural frequencies of the system (f_n) and others corresponding to the components $f_n \pm \Omega$ and $f_n \pm 2\Omega$.

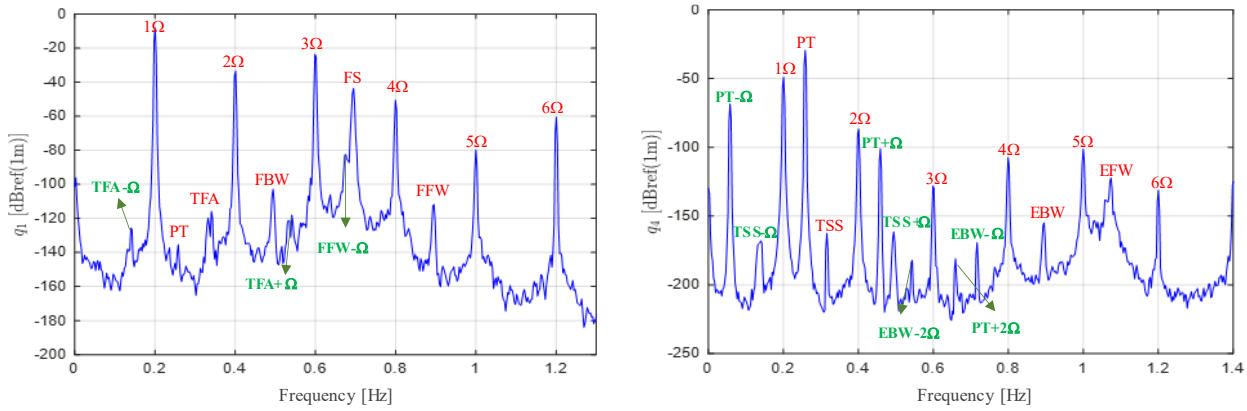

Figure 6. PSD of forced vibration response: on the left blade flapwise and on the right blade edgewise.

The results presented in this subsection are in good agreement with those simulated and measured presented by Allen et. *al.* (2011), Yang et *al.* (2014), and Requeson et *al.* (2015).

5.2.1 Vibration analysis using mbc

To filter most of the harmonic components that come along due to the time dependence of the system and obtain a better comprehension of the dynamics involved in the WT model, this section discusses the vibratory behavior of the wind turbine with the aid of the Multi-blade Coordinate Transformation.

The original system was integrated, and then, the MBC was applied only to the system's responses in DOF's that are defined in the rotating coordinate systems. Using Eq. (4), the DOFs associated with flapwise (q_1, q_2 e q_3) and edgewise (q_4, q_5 e q_6) movements were transformed into non-rotational coordinates q_0^f, q_c^f, q_s^f and q_0^e, q_c^e, q_s^e (Bir, 2008, 2010). These non-rotational coordinates represent a collective movement of the rotor blades: q_0^f is the collective and in-phase movement of all blades in flapwise, q_0^e, is the collective and in-phase movement of the rotor in edgewise. The coordinate q_c^f corresponds to the rotor longitudinal tilt moment about a horizontal line at the rotor plane, while q_s^f corresponds to the rotor lateral tilt moment about a vertical line at the rotor plane. Lastly, q_c^e and q_s^e describe, respectively, the horizontal and vertical movements of the rotor's mass center.

The PSDs of those signals are shown in Figures 7 to 9. The first characteristic to notice is that, as explained by Bir (2008, 2010), the MBC does not eliminate all periodic terms, especially the ones which are integer multiples of ΩN, therefore it does not transform a time-variant system to a time-invariant one.

Figure 7, on the left, shows the PSD of q_0^f, in which can be seen the modes that most contribute to rotor movement by this coordinate: symmetrical flapwise (FS), the fore-and-after of the tower (TFA) and the 2nd power train torsional mode (PT). Figure 7, on the right, shows the PSD of q_0^e, it is noticed that the 2nd power train's torsion mode is dominant in this case, the rotor's torsion mode couples to blade's edgewise movements leading them to bending in phase on the rotor plane, hence this configuration was expected.

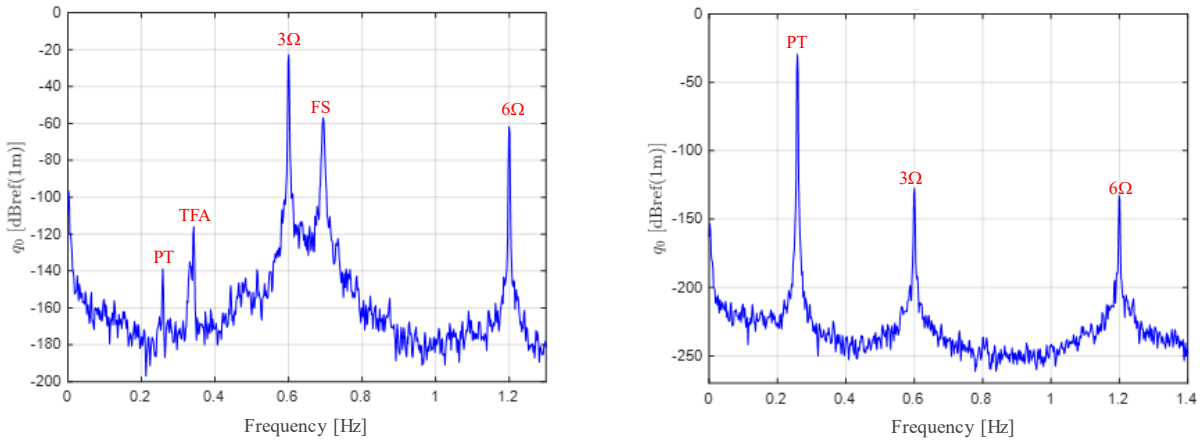

Figure 7. PSDs of q_0 flapwise, on the left, and q_0 edgewise, on the right.

Figures 8 show the PSDs of q_c^f and q_s^f, on the left and the right, respectively. Analyzing q_c^f, the contribution of all modes is also identified in the q_0^f analysis, however, in this PSD, the dominant modes (greatest frequencies peak among the WT natural frequencies) are those related to the rotor flapwise precession (FBW and FFW). Furthermore, the MBC had not filtered out the 1Ω harmonic frequency which indicates a slight anisotropy in the model.

Finally, the PSDs referring to q_c^e and q_s^e are shown in Figure 9, on the left and the right, respectively. It is observed that the frequency referring to the 2nd power train torsion is dominant due to the hard coupling between the rotor and blades, but the frequencies associated with edgewise precession frequencies (EFW and EBW) of the rotor exhibit considerable peak as well.

Analyzing the results presented in Figures 8 and 9, it is possible to observe that the application of MBC filtered out most of the harmonic components associated with rotation and eliminated most of the terms $f_n \pm n\Omega$, but not all. The component 1Ω appears both in the PSDs of the non-rotational coordinates associated with the flapwise (Figure 8) and in those that refer to the edgewise (Figure 9). Terms $f_n \pm n\Omega$ appear, predominantly, in the edgewise PSDs, however, those frequencies have amplitudes that are approximately 10^5 less than the dominant frequencies amplitude in PSD, which suggests that the anisotropy present in the model is small.

To a small degree, anisotropy directly affects the filtering operation performed when applying MBC, allowing the passage of a more significant number of harmonics (Bir, 2008; Bir, 2010), as occurred in the simulations presented in this work. Despite this, the results are consistent with the literature, especially with the measurements made by Requeson et *al.* (2015), which also exhibit harmonics due to the anisotropic nature of the wind turbine.

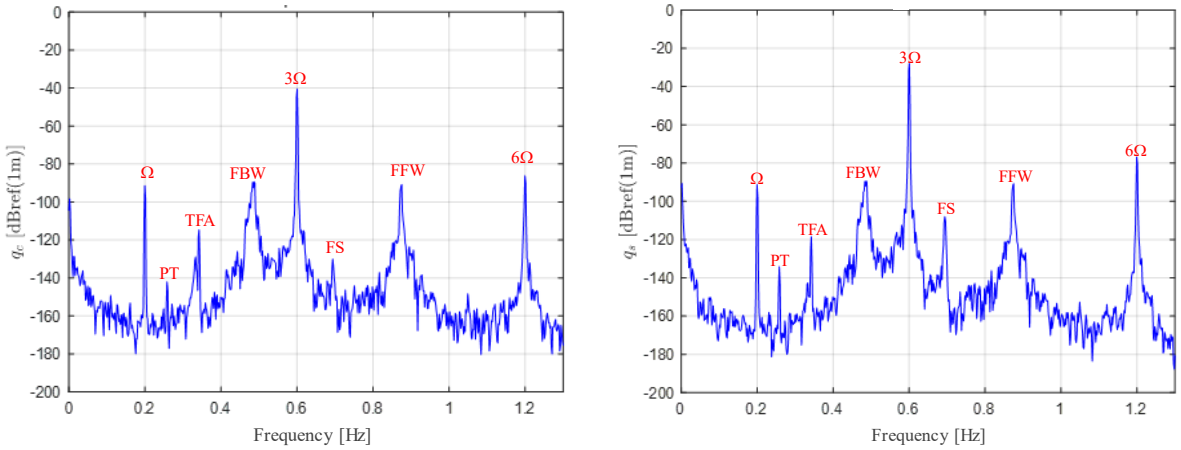

Figure 8. PSDs of flapwise coordinates: q_c^f on the left, and q_s^f on the right.

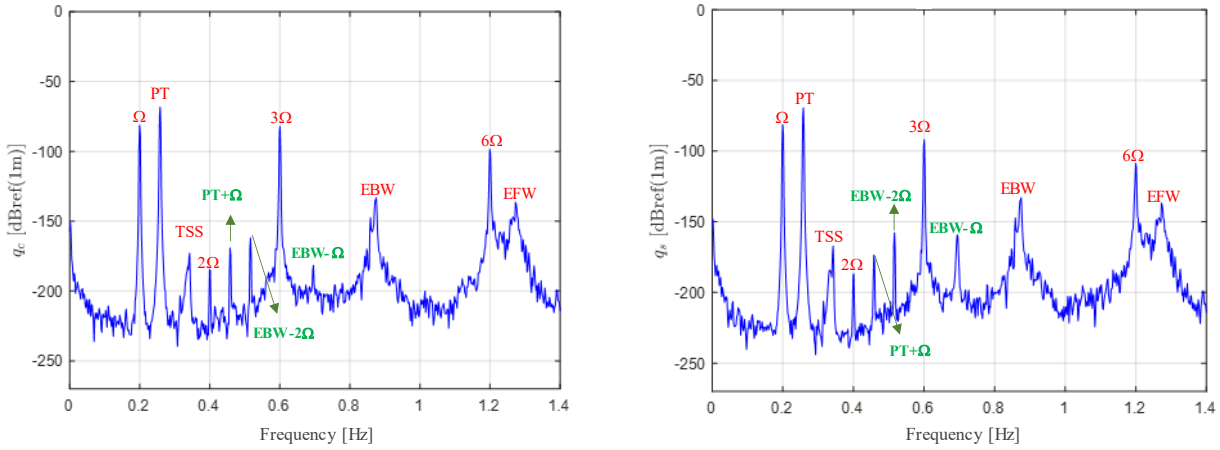

Figure 9. PSDs of edgewise coordinates: q_c^e on the left, and q_s^e on the right.

5. CONCLUSIONS

In this work, we implemented a wind turbine aeroelastic model with 13 DOF exposed to a two-dimensional turbulent wind field to analyze the low-frequency vibrations behavior. The three blades are modeled by Bernoulli-Euler Beam theory, the system was modeled using modal approach and the technical specifications are provided by NREL offshore 5-MW Baseline Wind Turbine.

The model periodic time-dependence was analyzed through impulse tests and the application of the Multi-Blade Coordinate Transformation. This transformation was applied to filter out periodic frequencies from the PSDs. The SANDIA Method was used to model the 2D turbulent wind field, and the difference between the point of view in the spectra (space frame or rotational blade frame) is analyzed. The PSD results show a considerable coupling between the model's degrees of freedom together with the periodic time-dependence presented by the model.

The model slightly anisotropy directly affected the MBC's filtering operation, allowing the passage of more significant harmonics. Harmonics components were more present in edgewise associated coordinates than in flapwise ones, and those results require further investigations. However, studies involving time-varying periodic systems and the impact of harmonic components related to the natural frequencies of the system on the modal behavior of wind turbines demand Fourier coefficients analysis for each mode together with the meticulous application of the Lyapunov–Floquet Transform. This leads to issues that incite quite wide-ranging discussions, which, therefore, are beyond the scope of this work.

Furthermore, all simulations performed in this work presented a good agreement with the simulated cases on literature and for field measures ones as well.

6. ACKNOWLEDGEMENTS

The authors would like to thank CAPES for the financial support.

7. REFERENCES

ABEEólica, 2019. *Boletim Anual de Geração Eólica, 2019.* Associação Brasileira de Energia Eólica, ABEEólica. http://abeeolica.org.br/wp-content/uploads/2020/06/PT_Boletim-Anual-de-Gera%C3%A7%C3%A3o-2019.pdf. Accessed 12 January 2021.

Allen M.S., Sracic M.W., Chauhan S., and Hansen M.H., 2011. "Output-Only Modal Analysis of Linear Time Periodic Systems with Application to Wind Turbine Simulation Data". *In: Proulx T. (eds) Structural Dynamics and Renewable Energy, Volume 1, Conference Proceedings of the Society for Experimental Mechanics Series*. Springer, New York, NY.

Bir, G, 2008. Multi-Blade *Coordinate Transformation and its Application to Wind Turbine Analysis - Proceedings of 2008 ASME Wind Energy Symposium Reno held in Nevada, USA, January 7-10, 2009.*

Bir, G., 2010. *User's Guide to MBC3 : Multi-Blade Coordinate Transformation Code for 3-Bladed Wind Turbines*. National Renewable Energy Laboratory. Available at: https://digitalscholarship.unlv.edu/renew_pubs/57/

Clough, R. W. and Penzien, J, 1975. *Dynamics of structures.* McGraw-Hill College, Auckland.

Hansen, M. H., 2016. "Modal dynamics of structures with bladed isotropic rotors and its complexity for 2-bladed rotors". *Wind Energy Science*. Vol. 1, p. 271-296.

IRENA, 2019. *Future of wind: Deployment, investment, technology, grid integration and socio-economic aspects, 2019,* International Renewable Energy Agency, IRENA. https://irena.org/-/media/Files/IRENA/Agency/%20Publication/2019/Oct/IRENA_Future_of_wind_2019.pdf . Accessed 12 January 2021.

Requeson, O. R., Tcherniak, D., and Larsen, G. C., 2015. "Comparative study of OMA applied to experimental and simulated data from an operating Vestas V27 wind turbine". *In Proceedings of the 6th International Operational Modal Analysis Conference – IOMAC 2015.* Gijón, Spain.

Skjoldan, P. F.; and Hansen, M. H, 2009. "On the similarity of the Coleman and Lyapunov-Floquet transformations for modal analysis of bladed rotor structures". *Journal of Sound and Vibration*, Vol. 374, p. 424–439.

Veers, P. S., 1988. *Three-dimensional Wind Simulation, Sandia Report*. Sandia National Laboratories, Albuquerque, New Mexico and Livermore, California.

Yang S., Tcherniak D., and Allen M.S., 2014. "Modal Analysis of Rotating Wind Turbine Using Multiblade Coordinate Transformation and Harmonic Power Spectrum*". In: De Clerck J. (eds) Topics in Modal Analysis I, Volume 7. Conference Proceedings of the Society for Experimental Mechanics Series*. Springer, Cham.

Zhang, Z, 2015. *Passive and Active Vibration Control of Renewable Energy Structures*. Doctoral Dissertation, Teknisk-Naturvidenskabelige Fakultet, Aalborg Universitet, Demanrk.

8. RESPONSIBILITY NOTICE

The authors are the only responsible for the printed material included in this paper.